

Growth of Straight, Atomically Perfect, Highly Metallic Silicon Nanowires with Chiral Asymmetry

Paola De Padova,^{*,†} Claudio Quaresima,[†] Paolo Perfetti,[†] Bruno Olivieri,[‡]
Christel Leandri,[§] Bernard Aufray,[§] Sebastien Vizzini,[§] and Guy Le Lay[§]

CNR-ISM, via Fosso del Cavaliere, 00133 Roma, Italy, CNR-ISAC, via Fosso del
Cavaliere, 00133 Roma, Italy, and CRMCN-CNRS, Campus de Luminy, Case 913,
13288 Marseille Cedex 9, France

Received October 8, 2007; Revised Manuscript Received November 30, 2007

ABSTRACT

In the quest of nano-objects for future electronics, silicon nanowires could possibly take over carbon nanotubes. Here we show the growth by self-organization of straight, massively parallel silicon nanowires having a width of 1.6 nm, which are atomically perfect and highly metallic conductors. Surprisingly, these silicon nanowires display a strong symmetry breaking across their widths with two chiral species that self-assemble in large left-handed and right-handed magnetic-like domains.

The opportunities offered by a wide range of nanowire (NW) materials with controlled chemical compositions, physical sizes, and electronic properties open many exciting prospects ranging from fundamental studies of the role of dimensionality on physical properties to potential applications in nanotechnology.^{1,2} Specifically, silicon nanowires (SiNWs) are one of the most challenging structures in nanoscience^{1–4} due to the central function played by Si in the world of the semiconductor industry; for future electronics and possibly quantum computing, silicon nanowires could play a key role and take over carbon nanotubes.¹ Several approaches have been developed for the growth of SiNWs such as laser ablation,⁵ metal-catalytic vapor–liquid–solid,⁶ oxide-assisted catalyst-free methods,⁷ as well as solution techniques.⁸

The potentiality of self-assembly used to organize spontaneously low-dimensional materials such as quantum dots and nanowires has been successfully applied recently to the formation of self-aligned straight SiNWs on the silver (110) surface.⁹ Room temperature (RT) deposition of a low coverage of Si on the Ag(110) surface produced massively parallel SiNWs sharing a common width of just ~ 16 Å, as shown by scanning tunneling microscopy (STM) measurements.⁹

Following this experimental finding, Guo-min He¹⁰ investigated in a recent theoretical study the adsorption of Si on the Ag(110) surface with the aim of elucidating the atomic

structure of these SiNWs; various adsorption geometries have been considered for Si coverages up to 2 monolayers (MLs). Although Si–Ag bonds are stronger than Si–Si bonds at low Si coverages, at higher Si coverages, the formation of Si dimers becomes instead more favorable yielding stable SiNWs on the Ag(110) surface at coverage of 1.2 ML, in the devised ground state structure (so-called g1).¹⁰ This structure presents strong similarity to that of the clean Si(001)- 2×1 reconstructed surface of paramount practical importance.¹¹ Two Si and two Ag layers are theoretically involved in the formation of these SiNWs: the top Si layer is formed by Si dimers and the second layer below is constituted of Si atoms in contact with the first and the second Ag layers. This tentative atomic model¹⁰ is particularly interesting in view of the fact that the Si dimers of the top layer appear to be symmetric, making the SiNWs intrinsically metallic, independently of any proximity effect. However, this theoretical model may be questionable since it does not explain, per se, the restriction to the ~ 16 Å unique width of the SiNWs. Experimentally, the metallic character of the SiNWs was especially revealed by the increased intensity at the Fermi level in angle-integrated valence band spectra and by the clear asymmetry of the Si 2p core level line shapes, confirmed by the high value of the asymmetry index of the Doniach–Sunjic function¹² used in their fitting procedure.⁹

We will show in this letter that the SiNWs present a surprising transverse asymmetry. Since, unfortunately, a detailed structural study is still lacking, the atomic structure

* To whom correspondence should be addressed. Tel: +39-06-49934144.
Fax: +39-06-49934153. E-mail: paola.depadova@ism.cnr.it.

[†] CNR-ISM.

[‡] CNR-ISAC.

[§] CRMCN-CNRS.

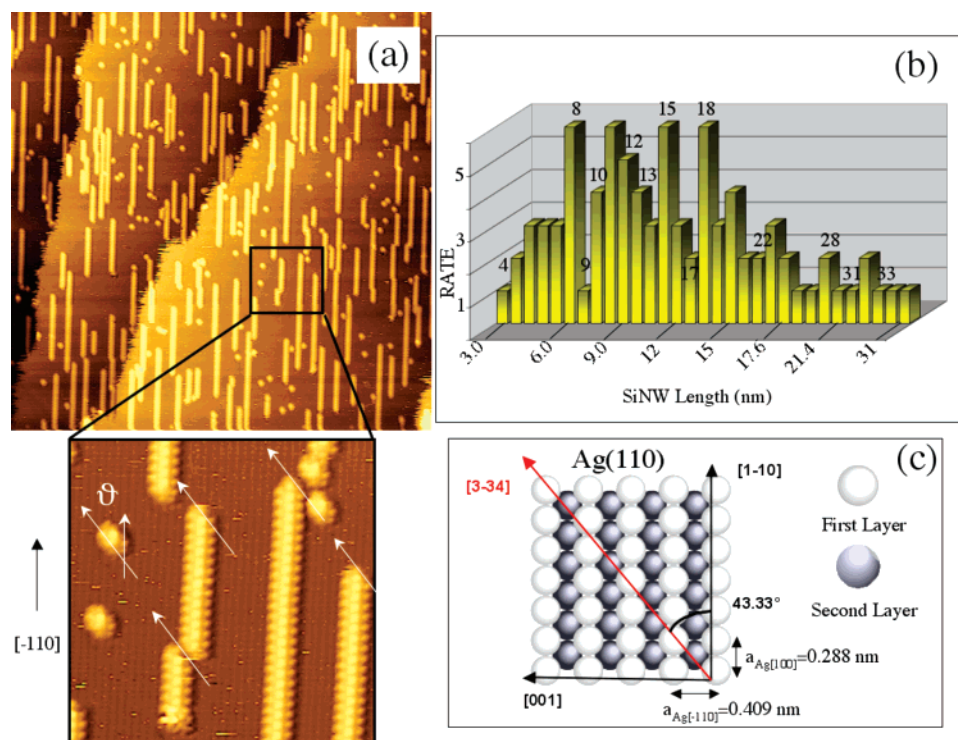


Figure 1. (a) 100×100 nm filled-states STM image of SiNWs on Ag(110) at RT; $V = -1.7$ V, $I = 1.14$ nA. (b) Histogram of the rate size-length distribution of SiNWs; (c) Draft of Ag(110) surface, the angle between the $[-110]$ and $[3-34]$ directions is 43.33° .

of these SiNWs is not yet known, not even the exact number of constitutive silicon atoms.

The Si 2p core level is the most widely investigated spectral feature in soft X-ray photoelectron spectroscopy, constituting a fundamental playground for solid-state physics research.^{13,14} Although remarkably narrow Si 2p core levels for the SiNWs were measured in the initial study,⁹ some of their basic properties have not been accurately determined. This is especially the case for the intrinsic Si 2p core hole lifetime Γ for each of the components associated with the different Si atoms involved in the formation of the nanowires.

We highlight in this letter two of these fundamental issues. First, a novel observation of STM topographic images reveals details of a surprising crystal symmetry breaking. Second, recording by high-resolution photoemission spectroscopy the narrowest Si 2p core levels ever measured in solid phase, we determine, for the first time, the different life times of the Si 2p_{1/2} and Si 2p_{3/2} core holes resulting from a Coster–Kronig transition¹⁵ forbidden in semiconductors, but allowed in metals, and in addition we identify two new silicon sites.

The STM observations of the SiNWs were carried out at the CRM-CN in Marseille, whereas the photoemission experiments were carried out at the VUV beamline of the Italian synchrotron radiation facility ELETTRA in Trieste. In both places, the same procedure has been used for sample preparation and silicon evaporation. The Ag(110) substrate was cleaned in the UHV chamber (base pressure: 8.5×10^{-11} mbar) by repeatedly sputtering with Ar⁺ ions and annealing the substrate at 750 K, while keeping the pressure below 2×10^{-10} mbar during the heating. Si was evaporated at a rate of ~ 0.03 ML/min from a Si source, while the Ag substrate was kept at room temperature (RT). This condition

has been shown to give definite LEED patterns, where, in addition to the sharp integer order spots of the unreconstructed Ag(110) surface, thin streaks elongated along the $[100]^*$ reciprocal direction, develop through the substrate spots as well as in half-order position along the perpendicular $[-110]^*$ direction. The silicon coverage was measured using a quartz microbalance; the error in determining the Si amount was estimated to be less than 10%. The sample temperature was measured by an infrared pyrometer. All STM images presented in the following were recorded at RT in constant-current mode at a bias voltage of -1.7 V and a tunneling current of 1.2 nA.

Figure 1a displays a 100×100 nm² filled-states STM image of ~ 0.5 ML Si deposited at RT on the Ag(110) surface, associated with a 15.8×15.8 nm² high-resolution zoom of the square area indicated. The large STM image consists of extended (110) terraces typical of stepped Ag(110) surfaces,¹⁶ with Si nanostructures on top, from nanodots to massively parallel SiNWS, all aligned along the $[-110]$ direction of the Ag(110) surface. Their lengths vary from 1.5 nm for the nanodots to 31 nm for the NWs. A histogram constructed from the rate of incidence of each SiNW length on a 100 nm² area (excluding the numerous 1.5 nm size nanodots) shows a Gaussian-like distribution peaked at ~ 10 nm. We note that the SiNWs are basically composed of an integer number of 1.5 nm size blocks, as indicated on top of the bars making the histogram of Figure 1b. This confirms that the SiNWs are constituted by the self-assembly of the individual nanodots seen on the figure.⁹

The zoom reveals details of the 1.5 nm dots and of the NWs' terminations. It is clearly noticeable that the nanostructures are never terminated along the $[100]$ Ag direction

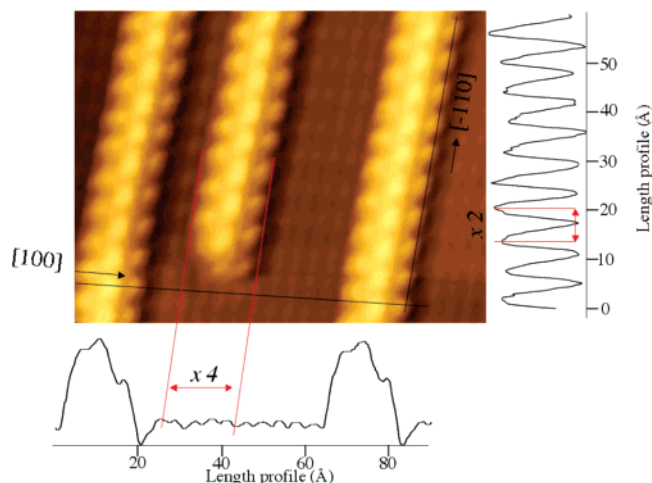


Figure 2. 10.2×10.2 nm² filled-states STM image. The line profiles indicate the $x2$ and $x4$ periodicity respectively parallel and perpendicular to the $[-110]$ direction.

(i.e., perpendicularly to the direction of the SiNWs) but along another definite orientation, which we assign to the $[3-34]$ direction of the Ag(110) surface. This fact confers to all nanodots, and of course also to all NWs, a surprising asymmetric morphology with respect to the plane perpendicular to the (110) surface.

Furthermore, the asymmetric transverse shape of the SiNWs is evidenced on the high magnification (10.2×10.2 nm²) STM image displayed in Figure 2. On this image, the atomic resolution obtained on the bare Ag(110) surface allows us to determine directly the $x2$ periodicity of the SiNWs parallel to the Ag direction (i.e., $2a_{\text{Ag}[-110]}$). One can further notice a misalignment between the right and left side protusions corresponding to a glide of one $a_{\text{Ag}[-110]}$ lattice parameter. The line profile along the perpendicular $[100]$ direction assigns a lateral size of ~ 1.6 nm for every single SiNW, i.e., an $x4$ width of $4a_{\text{Ag}[100]}$, where $a_{\text{Ag}[100]} = 0.409$ nm, whereas the height is about 0.2 nm.

Figure 3a displays a 3D view of the previous STM image (Figure 2). A dip is clearly noticeable on the right side of each NW. The line profile reveals the presence of a small slanted $(11-1)$ atomic facet oriented at 135° with respect to the (110) surface.¹⁷ We can definitely rule out that this feature is a tip-dependent artifact, because the effect was observed on all STM images collected on large areas both in forward and backward scans whatever the tip scan orientations and with several tips. The dip along each NW suggests that the Ag atoms from the missing row of the substrate could be part of the SiNWs, eventually inducing the crystal symmetry breaking. In this respect, we recall that silver likes to wet the silicon surfaces.¹⁸ This possibility is not included in the atomic model of Guo-minh He,¹⁰ which, however, favors the asymmetric model where the two dimer rows are shifted by one Ag–Ag interatomic distance along the $[-110]$ direction.

Surprisingly, in all previous figures, the dip is always on the right-hand side of the NWs. However, we stress that on other extended areas (see Figure 3b) we met the reverse situation where the dip is always situated on their left side

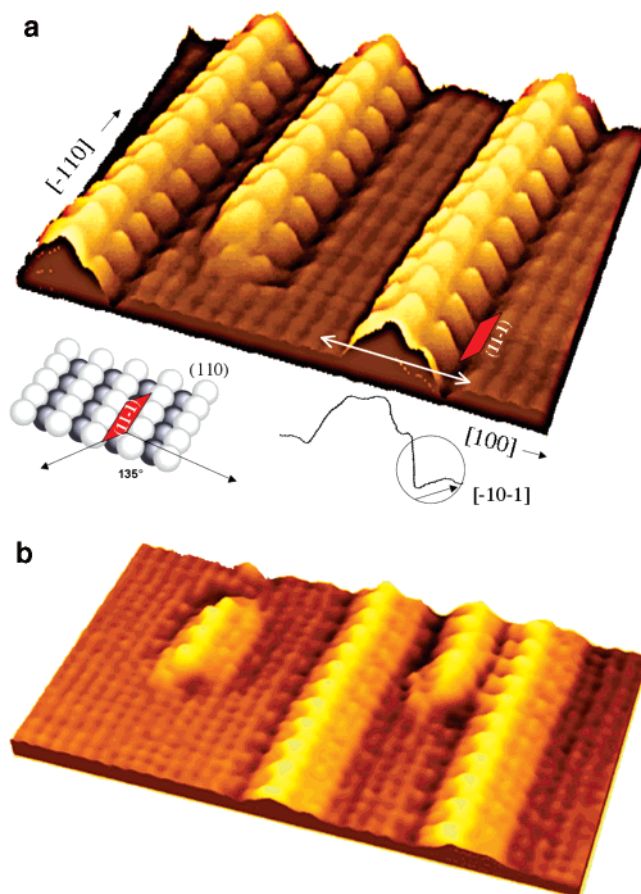


Figure 3. (a) 3D view of 10.2×10.2 nm² filled-states STM image: dip asymmetry at right-side. (b) 3D view of 10.2×10.2 nm² filled-states STM image: dip asymmetry at left-side.

and the nanostructures are terminated along the $[-334]$ direction, symmetric to the previous $[3-34]$ one. Hence, astonishingly, the two types of symmetry breaking NWs phase separate in large “magnetic-like” domains of opposite “spins” to recover the overall mirror symmetry of the bare surface. Unfortunately, we have not yet determined the domain boundary regions on the high-resolution STM image, where the asymmetry dip is visible, due to the large size of the left- and right-handed domains, which we estimate to be several microns per side. The “phase” condensation in two types of separate domains implies a cross talk between NWs having the same “spin”. This is confirmed by perusal at Figure 3a, where one can notice an $x2$ periodicity on the bare silver areas, as along the NWs themselves. This points to a strain-induced modulation of the substrate extending along the NWs and propagating to a certain distance perpendicularly. This “mattress” effect induces the cross-talk and favors the formation of separate domains because of the glide along the $[-110]$ direction mentioned above. We note that to the best of our knowledge such a chiral coupling between wires leading to large left- and right-handed domains has been only found for wires of organic molecules by Pascual et al.¹⁹

The photoemission spectra were recorded after cooling the sample to ~ 150 K. They were acquired using an angle-resolved electron energy analyzer with an acceptance of 2° .

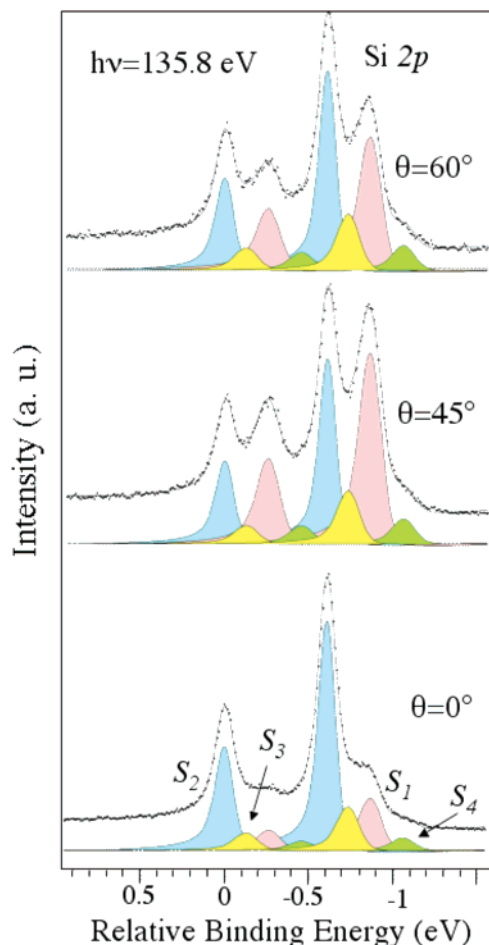


Figure 4. Normal ($\vartheta = 0^\circ$ and $\vartheta = 45^\circ$) and grazing ($\vartheta = 60^\circ$) emission convoluted Si 2p core levels for SiNWs after the deposition of 0.5 ML of Si on Ag(110).

For core level measurements, the angle between the photon beam and the normal to sample surface was 17° ; the collection angle $\vartheta = 0^\circ$ corresponds to normal emission. The photon energy was set to 135.8 eV, whereas the total energy resolution was better than 50 meV. Figure 4 displays high-resolution Si 2p core-level spectra measured at $\vartheta = 0^\circ$ (normal), 45° , and 60° electron emission angles from a corresponding, 0.5 ML Si deposited, Ag(110) surface at RT.

The figure clearly shows that the Si 2p peak is essentially composed of two (spin–orbit splitted) major components, yet smaller other contributions can also be noticed. More quantitative information is obtained by synthesizing the spectra with spin–orbit split Doniach–Sunijch (D–S) functions.¹² A least-square fitting procedure was used, with four doublets, each with a spin–orbit splitting of $609 \pm 5 \text{ meV}$, a branching ratio of 0.53, and an asymmetry parameter of 0.122, which indicates that the Si nanowires have a strong metallic character. This metallicity is also demonstrated by the two $I(V)$ spectra acquired either strictly on the NWs or on the bare Silver surface (see Figure 5).

The Si 2p core level collected at $\vartheta = 0^\circ$ is completely dominated by the S_2 component. Its full width at half maximum (FWHM) is only 130 meV. This is the narrowest Si 2p line shape ever reported in a solid-phase photoemission experiment, being narrower than the bulk line in a silicon

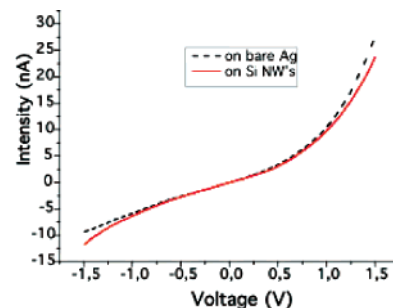


Figure 5. $I-V$ characteristic of 0.5 ML of Si on Ag(110).

single crystal.¹⁴ This result shows that the Si NWs are atomically precise objects and that the whole ensemble at macroscopic scale is practically free of defects. The best fit of all spectra at different collection angles is obtained with two small components S_3 and S_4 in addition to the major S_2 and S_1 ones. The S_1 component is located at -0.26 BE (we reference the BE to the position of the Si $2p_{1/2}$ line of the S_2 component) and shows colossal photoelectron diffraction effects at higher emission angles. The two new weak components S_3 and S_4 are respectively at -0.13 and -0.46 eV . At normal emission, the spectrum is dominated by S_2 . The result of its fit imposes two significantly different values of the Lorentzian FWHMs $\Gamma_{3/2} = 25 \text{ meV}$ and $\Gamma_{1/2} = 40 \text{ meV}$ respectively for the Si $2p_{3/2}$ and Si $2p_{1/2}$ lines, which have a common Gaussian FWHM of just 95 meV. The evidence of the extra broadening of the $2p_{1/2}$ Lorentzian FWHM, points to a nonradiative Coster–Kronig Auger LLV transition, forbidden in semiconducting Si (Si gap: 1.12 eV) but allowed in a metallic state. This is in agreement with the metallicity demonstrated from the $I(V)$ spectra and derived from the asymmetry parameter.

These $\Gamma_{1/2}$ and $\Gamma_{3/2}$ values are also used for the other components in all spectra, while the Gaussian FWHM of S_2 , S_3 , and S_4 was 135 meV.

The dominant intensity of S_2 at normal emission demonstrates that S_2 arises from Si atoms located at the bottom of the SiNWs at variance with what was erroneously attributed in ref 9. As a consequence S_1 is related to the top Si layer (let us recall that the STM line profile shows a corrugation of only $\approx 2 \text{ \AA}$). The ratio $R \approx 1$ between the S_1 and S_2 components at 45° emission indicates strong diffraction effects related to the SiNW atomic structure. The smaller S_3 and S_4 components can be attributed to different Si atoms located at the extremities of the SiNWs or to the nanodots, which are numerous on the Ag(110) surface. These results show that the structure of the SiNWs is probably more complicated than that proposed in He's model, ref 10. Work is in progress for the SiNWs structure determination.

However, for the two small additional components found here, we note that the resulting decomposition is in close agreement with that of ref 9, where just the two main components, S_1 and S_2 , were identified.

To summarize, we succeeded in growing at room-temperature straight, high aspect ratio silicon nanowires which lie in a massively parallel alignment. These objects appear atomically perfect, better than bulk silicon itself,

revealing a highly metallic character. Furthermore, they display a clear transverse symmetry breaking with two chiral species that, surprisingly, self-assemble in large left-handed and right-handed, “magnetic”-like domains.

Acknowledgment. The authors thank the staff of ELETTRA and of the VUV beam line.

References

- (1) Ma, D. D. D.; Lee, C. S.; Au, F. C. K.; Tong, S. Y.; Lee, S. T. *Science* **2003**, 299 (5614), 1874–1877.
- (2) Appell, D. *Nature* **2002**, 419 (6907), 553–555.
- (3) Huang, Y.; Duan, X.; Cui, Y.; Lieber, C. M. *Nano Lett.* **2002**, 2 (2), 101–104.
- (4) Bruno, M.; Palummo, M.; Marini, A.; Del Sole, R.; Ossicini, S. *Phys. Rev. Lett.* **2007**, 98 (3), 036807-1–036807-4.
- (5) Tang, Y. H.; Zhang, Y. F.; Wang, N.; Lee, C. S.; Han, X. D.; Bello, I.; Lee, S. T. *J. Appl. Phys.* **1999**, 85 (11), 7981–7983.
- (6) Lincoln, Yi Cui.; Lauhon, J.; Gudiksen, M. S.; Wang, J.; Lieber, C. M. *Appl. Phys. Lett.* **2001**, 78 (15), 2214–2216.
- (7) Gole, J. L.; Stout, J. D.; Rauch, W. L.; Wang, Z. L. *Appl. Phys. Lett.* **2000**, 76 (17), 2346–2348.
- (8) Holmes, J. D.; Johnston, K. P.; Doty, R. C.; Korgel, B. A. *Science* **2000**, 287 (5457), 1471–1473.
- (9) Leandri, C.; Le Lay, G.; Aufray, B.; Girardeaux, C.; Avila, C. J.; Davila, M. E.; Asensio, M. C.; Ottaviani, C.; Cricenti, A. *Surf. Sci. Lett.* **2005**, 574 (1), L9–L15.
- (10) He, Guo-min. *Phys. Rev. B* **2006**, 73 (3), 035311–1–035311–8.
- (11) Enta, Y.; Suzuki, S.; Kono, S. *Phys. Rev. Lett.* **1990**, 65 (21), 2704–2707.
- (12) Doniach, S.; Sunjic, M. *J. Phys. C* **1970**, 3 (2), 285–291.
- (13) Landemark, E.; Karlsson, C. J.; Chao, Y.-C.; Uhrberg, R. I. G. *Phys. Rev. Lett.* **1992**, 69 (10), 1588–1592.
- (14) De Padova, P.; Larciprete, R.; Quaresima, C.; Ottaviani, C.; Ressel, B.; Perfetti, P. *Phys. Rev. Lett.* **1998**, 81 (11), 2320–2323.
- (15) Coster, D.; Kronig, R. de L. *Physica* **1935**, 2 (1–12), 13–24.
- (16) Koch, R.; Schulz, J. J.; Rieder, K. H. *Eur. Phys. Lett.* **1999**, 48 (5), 554–560.
- (17) Fölsch, S.; Helms, A.; Zöphel, S.; Repp, J.; Meyer, G.; Rieder, K. H. *Phys. Rev. Lett.* **2000**, 84 (1), 123–126.
- (18) Le Lay, G. *Surf. Sci.* **1983**, 132 (1–3), 169–204.
- (19) Pascual, J. I.; Barth, J. V.; Ceballos, G.; Trimarchi, G.; De Vita, A.; Kern, K.; Rust, H.-P. *J. Chem. Phys.* **2004**, 120 (24), 11367–11370.

NL072591Y